AIAA JOURNAL
Vol. 33, No. 4, April 1995

Optimal Through-Thickness Temperature Gradients for Control of Interlaminar Stresses in Composites

Taehyoun Kim* and Satya N. Atluri†
Georgia Institute of Technology, Atlanta, Georgia 30332-0356

Analytical solutions are sought for optimal temperature distributions to control the interlaminar stresses near the free edges of composite laminates subjected to uniaxial loading. Optimal through-thickness temperature gradients are obtained by minimizing appropriate performance indices that are functions of the far-field properties, with respect to the through-thickness temperature differences. Through the application of these temperatures, effects of local mismatches as well as global mismatches in two of the elastic properties, the Poisson's ratio and coefficient of mutual influence, are minimized. Numerical examples are given for several lay-ups made of graphite epoxy. It is shown that for a cross- or angle-ply laminate a uniform temperature rise or drop can completely eliminate all of the interlaminar stresses, whereas for other laminates nonuniform temperature distributions must be applied to minimize the stresses.

Nomenclature

h = laminate thickness
M_{ij}^T = applied thermal moments (moment/unit length)
N = total number of plies
N_{ij}^T = applied thermal loads (force/unit length)
N_{11} = applied uniaxial loading (force/unit length)
$Q_{ij}^{(k)}$ = ply stiffness for the kth ply in the laminate axes
T_{ambient} = ambient temperature
$T_{\text{control}}^{(k)}$ = absolute temperature at the top of the kth ply as a control input
T_{zero} = zero residual stress temperature
$t^{(k)}$ = thickness of the kth ply
(x_1, x_2, x_3) = local coordinate system with the out-of-plane coordinate x_3 defined at the bottom of each ply
(x_1, x_2, z) = global coordinate system with the out-of-plane coordinate z defined at the midplane of the laminate
$z_3^{(k)}$ = global out-of-plane coordinate for the top of the kth ply
$\Delta T^{(k)}$ = temperature difference at the top of the kth ply
$\Delta \tilde{T}^{(k)}$ = actual temperature differences applied at the top of the kth ply as defined by Eq. (9)
$\Delta T^{(k)}(x_3)$ = temperature difference in the kth ply given as a function of through-thickness coordinate x_3
$\epsilon_{11}^{\text{mech}}$ = applied mechanical in-plane strain
$\boldsymbol{\epsilon}^{\text{tot}}$ = total in-plane strain vector at arbitrary plane
$\boldsymbol{\epsilon}_{11}^0$ = total in-plane strain vector at the midplane
$\bar{\eta}_{12,1}$ = laminate coefficient of mutual influence
$\eta_{12,1}^{(k)}$ = coefficient of mutual influence for the kth ply
$\eta_{12,1E}^{(k)}$ = equivalent coefficient of mutual influence for the kth ply
$\boldsymbol{\kappa}$ = total curvature vector
$\boldsymbol{\mu}^{(k)}$ = coefficient of thermal expansion vector for the kth ply in the laminate axes
$\bar{\nu}_{12}$ = laminate Poisson's ratio
$\nu_{12}^{(k)}$ = Poisson's ratio for the kth ply
$\nu_{12E}^{(k)}$ = equivalent Poisson's ratio for the kth ply
σ_{ij} = total stress components in tensor notation
$\tilde{\sigma}_{ij}$ = far-field stress components
$\bar{\sigma}_{ij}$ = stress components normalized by N_{11}/h

Received June 13, 1994; revision received Nov. 16, 1994; accepted for publication Nov. 18, 1994.

*Research Scientist, Computational Mechanics Center. Member AIAA.
†Institute Professor and Regents' Professor of Engineering, Computational Mechanics Center. Fellow AIAA.

I. Introduction

THE behavior of interlaminar stresses near free edges of composite laminates has been fairly well understood. Although large magnitudes of interlaminar stresses exist within distances of a few laminate thicknesses from the free edges, they are known to be causes of delamination that may lead to the fatal failure of composite structures under severe loading conditions.

In the literature, there has been a lack of research on the control of interlaminar stresses. Although various passive control strategies[1–3] have been suggested, they are often ineffective and may not be compatible with design goals. On the other hand, investigations on thermally induced stresses in composite laminates have revealed that edge effects induced by a uniform temperature change can result in interlaminar stresses of significant amounts.[4–6] This suggests that thermal loading, when applied with controlled magnitudes and spatial gradients, has the potential to compensate for the interlaminar stresses that have been caused by mechanical loading. Recently, Kim and Atluri[7] have shown that a thermomechanical control near the free edges with through-thickness temperature variations is indeed an efficient means for this purpose and provided analytical solutions for the optimal temperature distributions.

The present paper addresses a continuation of the work presented in Ref. 7 with added features including continuous, piecewise linear temperature distribution, a combined global-local optimization scheme, and use of a complete global-local-thermomechanical program in calculating the resulting interlaminar stress fields. For these purposes, an appropriate performance index that is to be minimized is defined in terms of the temperature gradients. Certain constraints such as that the temperature field must be smooth, or finite, can be incorporated into the minimization process. First, a global optimization including only global mismatch effects in the laminate is considered. Later, local mismatch effects are also included by considering a constrained optimization problem where a quadratic measure of the local mismatch terms is added as a constraint. Numerical examples are given for several graphite epoxy laminates subjected to uniaxial mechanical load and thermal gradients. The mechanical load is varied within the maximum first-ply-failure strength limit, and the feasibility of the thermomechanical control is examined. It is found that for a cross- or angle-ply laminate, a temperature rise or drop that is uniform throughout the laminate can completely eliminate all of the interlaminar stresses, whereas nonuniform temperature distributions must be applied to minimize the stresses in other types of laminates.

It is recognized that the precise implementation of the piecewise linear temperature gradients for general laminate lay-ups may not be possible in practice. Indeed, one may apply best at only one or two lamina interfaces, as, for instance, through nichrome wires[8] embedded at such interfaces. One then solves the heat conduction equation in the laminate to determine the temperature gradient throughout the laminate. Thus, in practice the presently determined optimal temperature gradients through the laminate thickness would be inputs to an inverse problem of heat conduction, to determine the heat input at one or more interfaces. Our experience in the lab indicates[8] that the heat input at interface, although not necessarily leading to temperature gradients that are mathematically optimal, would still lead to temperature gradients of a qualitative nature that are close enough to the optimum values to reduce the interlaminar stresses. Thus, until the inverse problem of heat conduction is solved, the present theoretical results provide guidelines as to where the heat should be introduced to reduce the interlaminar stresses, even in a nonoptimum way.

II. Classical Laminate Plate Theory

Classical laminate plate theory (CLPT) can be used to predict the far-field stresses under combined thermomechanical loading. For the analysis of the complete stress field, the following assumptions are made: the laminate is long enough in its longitudinal direction such that any longitudinal variations can be ignored; through-thickness temperature distribution is assumed to be piecewise linear within each lamina and continuous at all interfaces; and the laminate properties do not change with temperature variation. In addition, it is assumed that any temperature distribution can be specified and applied to control the interlaminar stresses. Thus, it is not necessary to consider the heat conduction equation and heat boundary conditions within the laminate.

According to the classical laminate plate theory, the global force resultant-strain relations in the interior region of the laminate, under a uniaxial loading N_{11} (force/length) and piecewise linear temperature distributions $\Delta T^{(i)}(z)$ $(i = 1, 2, \ldots, N)$ where i refers to the ith layer from the top of the laminate (see Fig. 1), are[9]

$$\begin{Bmatrix} N+N^T \\ M^T \end{Bmatrix} = \begin{bmatrix} A & B \\ B & D \end{bmatrix} \begin{Bmatrix} \epsilon^0 \\ \kappa \end{Bmatrix} \tag{1}$$

where A_{ij}, B_{ij}, and D_{ij} are the elements of the laminate stiffness matrix. The thermal load vector $N^T = [N_{11}^T\ N_{22}^T\ N_{12}^T]^T$ and the thermal moment vector $M^T = [M_{11}^T\ M_{22}^T\ M_{12}^T]^T$ are obtained via

$$N^T = \sum_{i=1}^{N} \int_{z^{(i+1)}}^{z^{(i)}} Q^{(i)} \mu^{(i)} \Delta T^{(i)}(z)\, dz \tag{2}$$

$$M^T = \sum_{i=1}^{N} \int_{z^{(i+1)}}^{z^{(i)}} Q^{(i)} \mu^{(i)} \Delta T^{(i)}(z) z\, dz \tag{3}$$

where $Q^{(i)}$ represents the ply stiffness matrix in the ith ply in the laminate axes. In the preceding expressions (2) and (3), the transition between the global z and the local x_3 is easily facilitated using the relation $z = z^{(k+1)} + x_3$ for the kth ply. (Except in a few definitions, the local coordinate x_3 is used throughout the present analysis.) Based on the piecewise linear approximation, the temperature distribution in each layer can be given in the local coordinate x_3 as

$$\Delta T^{(i)}(x_3) = a^{(i)} x_3 + b^{(i)} \tag{4}$$

where, for $0 < x_3 < t^{(i)}$ $(i = 1, 2, \ldots, N)$,

$$a^{(i)} \equiv \frac{\Delta T^{(i)} - \Delta T^{(i+1)}}{t^{(i)}}$$
$$b^{(i)} \equiv \frac{\Delta T^{(i+1)} z^{(i)} - \Delta T^{(i)} z^{(i+1)}}{t^{(i)}} \tag{5}$$

The stresses in the ith layer are related to the total strains via

$$\sigma^{(i)} = Q^{(i)} \left\{ \epsilon^{\text{tot}} - \mu^{(i)} \left[a^{(i)} x_3 + b^{(i)} \right] \right\} \tag{6}$$

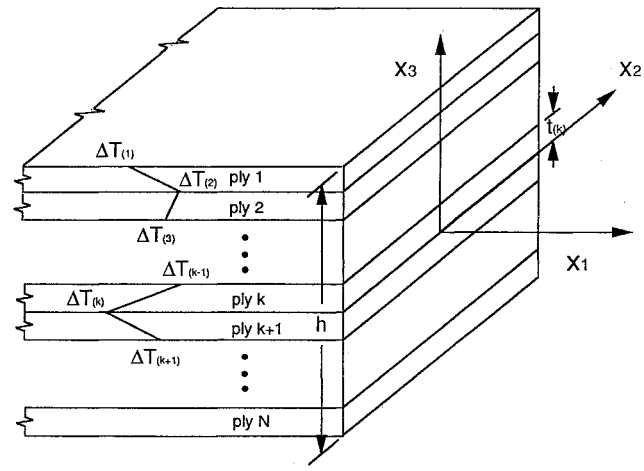

Fig. 1 Ply coordinate system.

The total strain vector in Eq. (6) is defined at an arbitrary plane and given as

$$\epsilon^{\text{tot}} = \epsilon^0 + z\kappa \tag{7}$$

where ϵ^0 and κ can be obtained by inverting the force resultant-strain relation (1).

It is recalled that the ith temperature difference (or gradient) is defined as

$$\Delta T^{(i)} \equiv T^{(i)}_{\text{control}} - T_{\text{zero}} \tag{8}$$

Therefore, the actual temperature differences that must be applied with respect to ambient temperature are

$$\Delta \tilde{T}^{(i)} = T^{(i)}_{\text{control}} - T_{\text{ambient}} = \Delta T^{(i)} + T_{\text{zero}} - T_{\text{ambient}} \tag{9}$$

III. Mechanical and Thermal Coefficients of Stresses

Under the assumption of the piecewise linear temperature distribution and the combined thermomechanical loading, the far-field in-plane stresses are at most linear in x_3. Thus, combining Eqs. (1), (6), and (7), one can write the far-field in-plane stress components in the kth layer as

$$\tilde{\sigma}_{11}^{(k)} = A_0^{(k)} + A_1^{(k)} x_3 \equiv A_{00}^{(k)} + A_{01}^{(k)} + \left[A_{10}^{(k)} + A_{11}^{(k)} \right] x_3 \tag{10}$$

$$\tilde{\sigma}_{22}^{(k)} = B_0^{(k)} + B_1^{(k)} x_3 \equiv B_{00}^{(k)} + B_{01}^{(k)} + \left[B_{10}^{(k)} + B_{11}^{(k)} \right] x_3 \tag{11}$$

$$\tilde{\sigma}_{12}^{(k)} = C_0^{(k)} + C_1^{(k)} x_3 \equiv C_{00}^{(k)} + C_{01}^{(k)} + \left[C_{10}^{(k)} + C_{11}^{(k)} \right] x_3 \tag{12}$$

In these expressions, the contribution from the thermal loading has been separated from that of mechanical loading. The first group of the coefficients $A_{00}^{(k)}$, $B_{00}^{(k)}$, $C_{00}^{(k)}$ and $A_{10}^{(k)}$, $B_{10}^{(k)}$, $C_{10}^{(k)}$ are proportional to the mechanical loading N_{11} and independent of temperature:

$$\begin{aligned} A_{00}^{(k)} &= \left[Q_{11}^{(k)} A_{11}^{-1} + Q_{12}^{(k)} A_{12}^{-1} + Q_{16}^{(k)} A_{13}^{-1} \right] N_{11} \\ B_{00}^{(k)} &= \left[Q_{12}^{(k)} A_{11}^{-1} + Q_{22}^{(k)} A_{12}^{-1} + Q_{26}^{(k)} A_{13}^{-1} \right] N_{11} \\ C_{00}^{(k)} &= \left[Q_{16}^{(k)} A_{11}^{-1} + Q_{26}^{(k)} A_{12}^{-1} + Q_{66}^{(k)} A_{13}^{-1} \right] N_{11} \end{aligned} \tag{13}$$

$$\begin{aligned} A_{10}^{(k)} &= \left[Q_{11}^{(k)} B_{11}^{-1} + Q_{12}^{(k)} B_{12}^{-1} + Q_{16}^{(k)} B_{13}^{-1} \right] N_{11} \\ B_{10}^{(k)} &= \left[Q_{12}^{(k)} B_{11}^{-1} + Q_{22}^{(k)} B_{12}^{-1} + Q_{26}^{(k)} B_{13}^{-1} \right] N_{11} \\ C_{10}^{(k)} &= \left[Q_{16}^{(k)} B_{11}^{-1} + Q_{26}^{(k)} B_{12}^{-1} + Q_{66}^{(k)} B_{13}^{-1} \right] N_{11} \end{aligned} \tag{14}$$

where A_{ij}^{-1}, B_{ij}^{-1}, and D_{ij}^{-1} are the elements of the laminate compliance matrix obtained as the inverse of the laminate stiffness

matrix defined in Eq. (1). The second group, $A_{01}^{(k)}, B_{01}^{(k)}, C_{01}^{(k)}$ and $A_{11}^{(k)}, B_{11}^{(k)}, C_{11}^{(k)}$, are independent of the mechanical loading but are linear functions of the temperature differences $\Delta T^{(i)}$ and can be written as

$$A_{01}^{(k)} \equiv \sum_{i=1}^{N+1} a_{A0i}^{(k)} \Delta T^{(i)}$$

$$B_{01}^{(k)} \equiv \sum_{i=1}^{N+1} a_{B0i}^{(k)} \Delta T^{(i)} \tag{15}$$

$$C_{01}^{(k)} \equiv \sum_{i=1}^{N+1} a_{C0i}^{(k)} \Delta T^{(i)}$$

and

$$A_{11}^{(k)} \equiv \sum_{i=1}^{N+1} a_{A1i}^{(k)} \Delta T^{(i)}$$

$$B_{11}^{(k)} \equiv \sum_{i=1}^{N+1} a_{B1i}^{(k)} \Delta T^{(i)} \tag{16}$$

$$C_{11}^{(k)} \equiv \sum_{i=1}^{N+1} a_{C1i}^{(k)} \Delta T^{(i)}$$

The various coefficients in these expressions, Eqs. (13–16), are defined in the Appendix.

IV. Global and Local Mismatches in the Elastic Properties

Although stress expressions in Eqs. (10–12) are convenient to use, they do not reveal individual contributions from mismatches in various elastic properties. To see these contributions clearly, let us consider a symmetric laminate under uniform stretching $\epsilon_{11}^{\text{mech}}$ and a symmetric layer-wise temperature distribution $\Delta T^{(i)}(x_3)$. In a composite laminate, the far-field in-plane stresses $\tilde{\sigma}_{22}^{(k)}$ and $\tilde{\sigma}_{12}^{(k)}$ will develop because of the mismatches between the individual ply strains and the global laminate strains. It can be shown that by relating the global and local strains to global and local Poisson's ratios and coefficients of mutual influence, respectively, the far-field stresses $\tilde{\sigma}_{22}^{(k)}$ and $\tilde{\sigma}_{12}^{(k)}$ can be written as

$$\tilde{\sigma}_{22}^{(k)} = \sum_{i=1}^{N+1} \left[a_{11i}^{(k)} Q_{12}^{(k)} + a_{22i}^{(k)} Q_{22}^{(k)} + a_{12i}^{(k)} Q_{26}^{(k)}\right] \Delta T^{(i)}$$
$$+ \left\{Q_{22}^{(k)}\left[\nu_{12}^{(k)} - \bar{\nu}_{12}\right] + Q_{26}^{(k)}\left[\bar{\eta}_{12,1} - \eta_{12,1}^{(k)}\right]\right\} \epsilon_{11}^{\text{mech}} \tag{17}$$

$$\tilde{\sigma}_{12}^{(k)} = \sum_{i=1}^{N+1} \left[a_{11,i}^{(k)} Q_{16}^{(k)} + a_{22,i}^{(k)} Q_{26}^{(k)} + a_{12,i}^{(k)} Q_{66}^{(k)}\right] \Delta T^{(i)}$$
$$+ \left\{Q_{26}^{(k)}\left[\nu_{12}^{(k)} - \bar{\nu}_{12}\right] + Q_{66}^{(k)}\left[\bar{\eta}_{12,1} - \eta_{12,1}^{(k)}\right]\right\} \epsilon_{11}^{\text{mech}} \tag{18}$$

Here the laminate Poisson's ratio $\bar{\nu}_{12}$ and the laminate coefficient of mutual influence $\bar{\eta}_{12,1}$ are defined as

$$\bar{\nu}_{12} = \frac{A_{12}A_{33} - A_{13}A_{23}}{A_{22}A_{33} - A_{23}^2} \tag{19}$$

$$\bar{\eta}_{12,1} = \frac{A_{12}A_{23} - A_{13}A_{22}}{A_{22}A_{33} - A_{23}^2} \tag{20}$$

and

$$\nu_{12}^{(k)} = \frac{Q_{12}^{(k)} Q_{66}^{(k)} - Q_{16}^{(k)} Q_{26}^{(k)}}{Q_{22}^{(k)} Q_{66}^{(k)} - Q_{26}^{(k)2}} \tag{21}$$

$$\eta_{12,1}^{(k)} = \frac{Q_{12}^{(k)} Q_{26}^{(k)} - Q_{16}^{(k)} Q_{22}^{(k)}}{Q_{22}^{(k)} Q_{66}^{(k)} - Q_{26}^{(k)2}} \tag{22}$$

and the coefficients $a_{11i}^{(k)}, a_{22i}^{(k)}, a_{12i}^{(k)}$ are defined in the Appendix. The preceding expressions now show three distinctive sources of the in-plane stress components: the global Poisson's ratio mismatches $\nu_{12}^{(k)} - \bar{\nu}_{12}$, the global coefficient of mutual influence mismatches $\bar{\eta}_{12,1} - \eta_{12,1}^{(k)}$, and the temperature gradients $\Delta T^{(i)}$ (the mechanical parts are identical to those derived in Ref. 10). The interlaminar stresses arise due to steep transverse gradients in $\sigma_{22}^{(k)}, \sigma_{12}^{(k)}$ near the free edges, whose free edge values are zero and far-field values are given by Eqs. (17) and (18) away from the edges. Therefore, these new stress equations imply that by applying a proper layer-wise temperature distribution, one can minimize the effects of the mismatches and reduce the level of the far-field in-plane stresses, thereby the interlaminar stresses.

The thermomechanical Eqs. (17) and (18) can be transformed to equivalent mechanical ones as follows:

$$\tilde{\sigma}_{22}^{(k)} = \left\{Q_{22}^{(k)}\left[\nu_{12E}^{(k)} - \bar{\nu}_{12E}\right] + Q_{26}^{(k)}\left[\bar{\eta}_{12,1E} - \eta_{12,1E}^{(k)}\right]\right\} \epsilon_{11}^{\text{tot}} \tag{23}$$

$$\tilde{\sigma}_{12}^{(k)} = \left\{Q_{26}^{(k)}\left[\nu_{12E}^{(k)} - \bar{\nu}_{12E}\right] + Q_{66}^{(k)}\left[\bar{\eta}_{12,1E} - \eta_{12,1E}^{(k)}\right]\right\} \epsilon_{11}^{\text{tot}} \tag{24}$$

where the new equivalent global and local Poisson's ratios and coefficients of mutual influence are defined, respectively, as follows:

Global:

$$\bar{\nu}_{12E} = -\frac{\epsilon_{22}^{\text{tot}}}{\epsilon_{11}^{\text{tot}}} \tag{25}$$

$$\bar{\eta}_{12,1E} = \frac{\gamma_{12}^{\text{tot}}}{\epsilon_{11}^{\text{tot}}} \tag{26}$$

Local:

$$\nu_{12E}^{(k)} = \nu_{12}^{(k)} \left\{1 - \frac{1}{\epsilon_{11}^{\text{tot}}} \left[\mu_{\alpha}^{(k)} + \frac{\mu_{\beta}^{(k)}}{\nu_{12}^{(k)}}\right] \Delta T^{(k)}(x_3)\right\} \tag{27}$$

$$\eta_{12,1E}^{(k)} = \eta_{12,1}^{(k)} \left\{1 - \frac{1}{\epsilon_{11}^{\text{tot}}} \left[\mu_{\alpha}^{(k)} - \frac{\mu_{\alpha\beta}^{(k)}}{\eta_{12,1}^{(k)}}\right] \Delta T^{(k)}(x_3)\right\} \tag{28}$$

In estimating the interlaminar stresses near the free edges, Rose and Herakovich[11] have shown that one must also take into account any possible local mismatches that may further exist between adjacent plies. For the combined thermomechanical problem, the local mismatches between the kth and the $(k+1)$th plies can be defined as

$$\delta\nu_{12E}(k) = \nu_{12E}^{(k)} - \nu_{12E}^{(k+1)} \tag{29}$$

$$\delta\eta_{12,1E}(k) = \eta_{12,1E}^{(k)} - \eta_{12,1E}^{(k+1)} \tag{30}$$

with $\delta\nu_{12E}(N) = \delta\eta_{12,1E}(N) = 0$. These mismatches affect the interlaminar stresses near the free edge region and do not appear in the far-field equations represented by Eqs. (23) and (24). However, their degrees of influences can be determined only in the context of energy principle. Reference 10 considers two nondimensional properties, $\delta\nu_{12}(k)\,\epsilon_{11}^{\text{mech}}$ and $\delta\eta_{12,1}(k)\,\epsilon_{11}^{\text{mech}}$, at each interface for the mechanical loading problem. For the combined thermomechanical problem the following mismatch quantities are considered for the kth ply:

$$\delta\nu_{12E}(k)\epsilon_{11}^{\text{tot}} = \delta\nu_{12}(k)\epsilon_{11}^{\text{tot}} - \delta a_{\nu\mu}(k)\,\Delta T^{(k+1)} \tag{31}$$

$$\delta\eta_{12,1E}(k)\epsilon_{11}^{\text{tot}} = \delta\eta_{12,1}(k)\epsilon_{11}^{\text{tot}} - \delta a_{\eta\mu}(k)\,\Delta T^{(k+1)} \tag{32}$$

where

$$\delta\nu_{12}(k) \equiv \nu_{12}^{(k)} - \nu_{12}^{(k+1)} \tag{33}$$

$$\delta\eta_{12,1}(k) \equiv \eta_{12,1}^{(k)} - \eta_{12,1}^{(k+1)} \tag{34}$$

$$\delta a_{\nu\mu}(k) \equiv \left[\nu_{12}^{(k)}\mu_{\alpha}^{(k)} + \mu_{\beta}^{(k)}\right] - \left[\nu_{12}^{(k+1)}\mu_{\alpha}^{(k+1)} + \mu_{\beta}^{(k+1)}\right] \tag{35}$$

$$\delta a_{\eta\mu}(k) \equiv \left[\eta_{12,1}^{(k)}\mu_{\alpha}^{(k)} - \mu_{\alpha\beta}^{(k)}\right] - \left[\eta_{12,1}^{(k+1)}\mu_{\alpha}^{(k+1)} - \mu_{\alpha\beta}^{(k+1)}\right] \tag{36}$$

For the case of general laminates where the combination of stacking sequences and thermal gradients can produce stretching-bending or stretching-twist couplings, one must take into account linear variation in the through-thickness direction in $\epsilon_{11}^{\text{tot}}$ and consider new local mismatch quantities as follows:

$$\delta\nu_{12E}(k)\,\epsilon_{11}^{\text{tot}(k)}, \qquad \delta\eta_{12,1E}(k)\epsilon_{11}^{\text{tot}(k)} \tag{37}$$

where $\epsilon_{11}^{\text{tot}(k)}$ now represents the total strain at the bottom of the kth ply.

V. Objective Functions and Minimization

A. Unconstrained Global Optimization

An appropriate performance index that is to be minimized is defined in terms of the through-thickness temperature gradients. The first performance index considered in this paper is

$$J_1 = \int_{-\frac{h}{2}}^{\frac{h}{2}} \left(\alpha\tilde{\sigma}_{22}^2 + \beta\tilde{\sigma}_{12}^2\right) \mathrm{d}z \tag{38}$$

where α and β are the weighting factors associated with the far-field in-plane stresses $\tilde{\sigma}_{22}$ and $\tilde{\sigma}_{12}$, respectively. This objective function is chosen based on the observation given in the previous section. That is, by minimizing the far-field in-plane stresses through application of a layer-wise temperature distribution, one can ensure that the interlaminar stresses will be also minimized. Note that this optimization scheme does not include local mismatch effects. The weighting factors α and β could be given as functions of x_3. However, they are set to be positive and constants in this study. The performance index can be rewritten in terms of the various coefficients defined in Eqs. (13–16):

$$\begin{aligned} J_1 = \sum_{k=1}^{N} \Big(\alpha\Big\{&\left[B_{00}^{(k)} + B_{01}^{(k)}\right]^2 t^{(k)} + \left[B_{00}^{(k)} + B_{01}^{(k)}\right] \\ &\times \left[B_{10}^{(k)} + B_{11}^{(k)}\right] t^{(k)2} + \tfrac{1}{3}\left[B_{10}^{(k)} + B_{11}^{(k)}\right]^2 t^{(k)3}\Big\} \\ &+ \beta\Big\{\left[C_{00}^{(k)} + C_{01}^{(k)}\right]^2 t^{(k)} + \left[C_{00}^{(k)} + C_{01}^{(k)}\right] \\ &\times \left[C_{10}^{(k)} + C_{11}^{(k)}\right] t^{(k)2} + \tfrac{1}{3}\left[C_{10}^{(k)} + C_{11}^{(k)}\right]^2 t^{(k)3}\Big\}\Big) \end{aligned} \tag{39}$$

Hence, taking derivatives of J_1 with respect to the $(N+1)$ temperature differences $\Delta T^{(i)}$ and setting them equal to zero, one obtains the following $(N+1)$ linear simultaneous equations:

$$\boldsymbol{B}\cdot\boldsymbol{\Delta T} = \boldsymbol{d} \tag{40}$$

where the elements of $(N+1)\times(N+1)\boldsymbol{B}$ and $(N+1)\times 1\boldsymbol{d}$ are obtained as

$$\begin{aligned} b_{ij} = \alpha \sum_{k=1}^{N} \Big\{&\left[2a_{B0j}^{(k)} t^{(k)} + a_{B1j}^{(k)} t^{(k)2}\right] a_{B0i}^{(k)} + \left[a_{B0j}^{(k)} t^{(k)2}\right. \\ &\left. + \tfrac{2}{3} a_{B1j}^{(k)} t^{(k)3}\right] a_{B1i}^{(k)}\Big\} + \beta \sum_{k=1}^{N} \Big\{\left[2a_{C0j}^{(k)} t^{(k)} + a_{C1j}^{(k)} t^{(k)2}\right] a_{C0i}^{(k)} \\ &+ \left[a_{C0j}^{(k)} t^{(k)2} + \tfrac{2}{3} a_{C1j}^{(k)} t^{(k)3}\right] a_{C1i}^{(k)}\Big\} \quad (i, j = 1, 2, \ldots, N+1) \end{aligned} \tag{41}$$

$$\begin{aligned} d_i = -\alpha \sum_{k=1}^{N} \Big\{&\left[2B_{00}^{(k)} t^{(k)} + B_{10}^{(k)} t^{(k)2}\right] a_{B0i}^{(k)} + \left[B_{00}^{(k)} t^{(k)2}\right. \\ &\left. + \tfrac{2}{3} B_{10}^{(k)} t^{(k)3}\right] a_{B1i}^{(k)}\Big\} - \beta \sum_{k=1}^{N} \Big\{\left[2C_{00}^{(k)} t^{(k)} + C_{10}^{(k)} t^{(k)2}\right] a_{C0i}^{(k)} \\ &+ \left[C_{00}^{(k)} t^{(k)2} + \tfrac{2}{3} C_{10}^{(k)} t^{(k)3}\right] a_{C1i}^{(k)}\Big\} \quad (i = 1, 2, \ldots, N+1) \end{aligned} \tag{42}$$

The forcing terms d_i are proportional to the load level, whereas the b_{ij} on the left hand side are load independent. Therefore, as long as the laminate properties are assumed invariant under temperature changes, the optimal temperature fields should vary linearly with the amount of the uniaxial load applied.

B. Constrained Global Optimization

Depending on perties and a stacking sequence of the laminate, a temperature field may be obtained that is not realizable in practice. To obtain temperature fields that are more feasible and less severe in distributions, a proper set of constraints must be introduced in the optimization procedure. In this section, a constraint that does not limit the sign of the temperatures but constrains their magnitudes is considered.

An obvious and simple choice would be that the weighted euclidean norm of temperature vector $\boldsymbol{\Delta T}$ be finite or

$$G = \sum_{i=1}^{N+1} \Delta T^{(i)2} w_i - R^2 = 0 \tag{43}$$

where $w_1, \ldots, w_{N+1}$ are fixed positive weighting numbers, and R is a norm of the weighted temperature vector. Both w_i and R are chosen a priori. Introducing the Lagrange multiplier λ, one can define a new objective function as

$$J_1^* = J_1 + \lambda G \tag{44}$$

Minimizing J_1^* with respect to $\Delta T^{(i)}$ leads to new set of $(N+1)$ linear equations in $(N+2)$ unknowns:

$$\boldsymbol{B}^*(\lambda)\cdot\boldsymbol{\Delta T} = \boldsymbol{d} \tag{45}$$

where the elements of the new $\boldsymbol{B}^*$ are defined as

$$b_{ij}^* = \begin{cases} b_{ij} & \text{if } i \neq j \\ b_{ii} + 2\lambda w_i & \text{if } i = j \end{cases} \tag{46}$$

and $\boldsymbol{d}$ is defined as before by Eq. (42). Equations (43) and (45) can now be solved for the $(N+2)$ unknowns $\Delta T^{(i)} (i = 1, 2, \ldots, N+1)$ and λ.

C. Combined Global-Local Optimization

With the exceptions of cross-ply and angle-ply laminates, the global minimization may not necessarily lead to a local minimization, and vice versa. To take further the local mismatches into account, one must add a quadratic measure of these mismatches to the performance index (38). To include the relative effects of global and local minimizations in one combined minimization, it is desirable that the local mismatch terms be added as a constraint in the optimization scheme. For this purpose, the following new index is considered:

$$J_2 = J_1 + \bar{\lambda} H \tag{47}$$

where

$$\begin{aligned} H = \gamma \sum_{k=1}^{N} \int_0^{l^{(k)}} &\left[\delta\nu_{12E}(k,1)\epsilon_l^{(k)} f_1^{(k)}(x_3)\right. \\ &+ \delta\nu_{12E}(k,2)\epsilon_b^{(k)} f_2^{(k)}(x_3)\Big]^2 \mathrm{d}x_3 \\ &+ \rho \sum_{k=1}^{N} \int_0^{l^{(k)}} \left[\delta\eta_{12,1E}(k,1)\epsilon_l^{(k)} g_1^{(k)}(x_3)\right. \\ &\left. + \delta\eta_{12,1E}(k,2)\epsilon_b^{(k)} g_2^{(k)}(x_3)\right]^2 \mathrm{d}x_3 - r^2 = 0 \end{aligned} \tag{48}$$

where $(k,1)$ and $(k,2)$ represent the top and bottom of the kth ply, respectively, and $\epsilon_l^{(k)}$ and $\epsilon_b^{(k)}$ [$= \epsilon_{11}^{\text{tot}(k)}$ in Eq. (37)] represent the total (mechanical plus thermal) extensional strain at the top and

bottom of the kth ply, respectively. The through-thickness weightings $f_1^{(k)}$, $f_2^{(k)}$, $g_1^{(k)}$, and $g_2^{(k)}$ are defined as

$$\begin{aligned} f_1^{(k)}(x_3) &= \frac{3x_3^2}{t^{(k)2}} - \frac{2x_3}{t^{(k)}} \\ f_2^{(k)}(x_3) &= \frac{3x_3^2}{t^{(k)2}} - \frac{4x_3}{t^{(k)}} + 1 \\ g_1^{(k)}(x_3) &= \frac{x_3^2}{t^{(k)2}} \\ g_2^{(k)}(x_3) &= \left[1 - \frac{x_3}{t^{(k)}}\right]^2 \end{aligned} \tag{49}$$

The preceding constraint H has been chosen based on the assumed through-thickness distributions of stresses due to the local mismatches in the equivalent Poisson ratios and coefficients of mutual influence.[10–12] The terms γ and ρ are weighting factors for the local mismatches, and r is the norm of the local quadratic measure. In fact, Ref. 11 discusses two types of Poisson mismatch effects at a ply interface. The first type, which is employed in the preceding text, is a direct result in the interlaminar shear stress $\sigma_{23}^{(k)}$, and the second one is a direct result in the interlaminar normal stress $\sigma_{33}^{(k)}$. For brevity, the present optimization scheme (48) includes only the first kind, but the second type of mismatch effect can be incorporated and added in a similar fashion, if one desires so. All of the γ, ρ, and r are set a priori, and they reflect how much the local mismatches should be minimized compared with the global mismatches. Minimization of J_2 leads to the following new set of $(N+1)$ linear simultaneous equations:

$$\boldsymbol{B}^{**}(\bar{\lambda})\cdot\boldsymbol{\Delta T} = \boldsymbol{d}^{**}(\bar{\lambda}) \tag{50}$$

where the elements of the new $\boldsymbol{B}^{**}$ and $\boldsymbol{d}^{**}$ are defined as

$$\begin{aligned} b_{ij}^{**} &= b_{ij} + \bar{\lambda} b_{hij} \\ d_i^{**} &= d_i + \bar{\lambda} d_{hi} \end{aligned} \tag{51}$$

where

$$\begin{aligned} b_{hij} \equiv \frac{\gamma}{15}\sum_{k=1}^{N} & [4\delta(a_{\nu 12})_i(k,1)\delta(a_{\nu 12})_j(k,1) \\ & + 4\delta(a_{\nu 12})_i(k,2)\delta(a_{\nu 12})_j(k,2) \\ & - \delta(a_{\nu 12})_i(k,1)\delta(a_{\nu 12})_j(k,2) \\ & - \delta(a_{\nu 12})_i(k,2)\delta(a_{\nu 12})_j(k,1)]t^{(k)} \\ & + \frac{\rho}{5}\sum_{k=1}^{N}[2\delta(a_{\eta 12,1})_i(k,1)\delta(a_{\eta 12,1})_j(k,1) \\ & + 2\delta(a_{\eta 12,1})_i(k,2)\delta(a_{\eta 12,1})_j(k,2) \\ & + \tfrac{1}{3}\delta(a_{\eta 12,1})_i(k,1)\delta(a_{\eta 12,1})_j(k,2) \\ & + \tfrac{1}{3}\delta(a_{\eta 12,1})_i(k,2)\delta(a_{\eta 12,1})_j(k,1)]t^{(k)} \end{aligned} \tag{52}$$

$$\begin{aligned} d_{hi} \equiv -\frac{\gamma}{15}\sum_{k=1}^{N} & \left[4\delta\nu_{12}(k,1)\delta(a_{\nu 12})_i(k,1)\epsilon_l^{\text{mech}(k)}\right. \\ & + 4\delta\nu_{12}(k,2)\delta(a_{\nu 12})_i(k,2)\epsilon_b^{\text{mech}(k)} \\ & - \delta\nu_{12}(k,2)\delta(a_{\nu 12})_i(k,1)\epsilon_l^{\text{mech}(k)} \\ & \left. - \delta\nu_{12}(k,1)\delta(a_{\nu 12})_i(k,2)\epsilon_b^{\text{mech}(k)}\right]t^{(k)} \\ & - \frac{\rho}{5}\sum_{k=1}^{N}\left[2\delta\eta_{12,1}(k,1)\delta(a_{\eta 12,1})_i(k,1)\epsilon_l^{\text{mech}(k)}\right. \\ & + 2\delta\eta_{12,1}(k,2)\delta(a_{\eta 12,1})_i(k,2)\epsilon_b^{\text{mech}(k)} \\ & + \tfrac{1}{3}\delta\eta_{12,1}(k,2)\delta(a_{\eta 12,1})_i(k,1)\epsilon_l^{\text{mech}(k)} \\ & \left. + \tfrac{1}{3}\delta\eta_{12,1}(k,1)\delta(a_{\eta 12,1})_i(k,2)\epsilon_b^{\text{mech}(k)}\right]t^{(k)} \end{aligned} \tag{53}$$

where $\epsilon_l^{\text{mech}(k)}$ and $\epsilon_b^{\text{mech}(k)}$ are the mechanical part of the total strains defined by Eq. (7) at the top and bottom of the kth ply, respectively, and the coefficients $\delta(a_{\nu 12})_i$ (k, 1 or 2) and $\delta(a_{\eta 12,1})_i$ (k, 1 or 2) are defined in the Appendix. Equation (50) and the constraint Eq. (48) can be solved simultaneously.

The combined global-local optimization can be further combined with any of the temperature constraints discussed previously, for example, Eq. (43), to give a constraint on the temperature field.

VI. Special Cases—Cross- and Angle-Ply Laminates

The cases of cross and angle plies merit particular attention since the expressions for the optimal temperatures simplify significantly. Because of its uniform stacking structure, a cross-ply or an angle-ply laminate allows the global and local equivalent mismatches to increase or decrease by the same ratio as functions of a uniform temperature difference ΔT. Therefore, it can be expected that, at a critical uniform temperature difference, both the global and local mismatch terms will disappear exactly. For these laminates, more insight can be gained by examining the basic equations rather than solving the optimization problem directly.

First, for a cross-ply laminate, there is no in-plane shear stress $\tilde{\sigma}_{12}$ at the far field. As a result,

$$C_{00}^{(k)} = C_{01}^{(k)} = C_{10}^{(k)} = C_{11}^{(k)} = 0 \tag{54}$$

Also, since the laminate is symmetric about its midplane,

$$A_{10}^{(k)} = A_{11}^{(k)} = B_{10}^{(k)} = B_{11}^{(k)} = 0 \tag{55}$$

Since σ_{22} is the only in-plane stress whose spatial gradient contributes to out-of-plane stresses, its minimization would lead to the minimization of the interlaminar stresses. By equating Eq. (17) for $\tilde{\sigma}_{22}^{(k)}$ to zero for any two consecutive k, i.e., for 90- and 0- or 0- and 90-deg plies, it can be shown that for both ply angles, hence for all plies, a uniform temperature can eliminate the in-plane stress $\sigma_{22}^{(k)}$. For a given mechanical strain $\epsilon_{11}^{\text{mech}}$, this unconstrained optimal temperature difference can be written in terms of basic uniply properties as follows:

$$\Delta T_{\text{cross,opt}} = \frac{(\bar{\nu}_{12} - \nu_{LT})\epsilon_{11}^{\text{mech}}}{A(\mu_L - \mu_T)} \tag{56}$$

where

$$A = \frac{E_L\left(E_L + E_T - 2E_T\nu_{LT} - E_T\nu_{LT}^2\right) + E_T^2\nu_{LT}^2(2\nu_{LT} - 1)}{E_L^2 + E_T^2 + 2\left(E_L E_T - 2E_T^2\nu_{LT}^2\right)} \tag{57}$$

where the subscripts L and T represent the longitudinal and transverse direction of a uniply, respectively. Thus, interlaminar stresses $\sigma_{33}^{(k)}$ and $\sigma_{23}^{(k)}$ in a cross-ply laminate can be completely eliminated by the optimal temperature given by Eq. (56).

For an angle-ply laminate, there is no in-plane normal stress $\tilde{\sigma}_{22}$ at the far field. As a result,

$$B_{00}^{(k)} = B_{01}^{(k)} = B_{10}^{(k)} = B_{11}^{(k)} = A_{10}^{(k)} = A_{11}^{(k)} = C_{10}^{(k)} = C_{11}^{(k)} = 0 \tag{58}$$

The only out-of-plane stress in this case is $\sigma_{13}^{(k)}$. By the same analogy used for a cross ply, it can be shown that a uniform temperature field will minimize the out-of-plane stress σ_{13} to zero. The unconstrained optimal temperature distribution for an angle-ply laminate can be written as (for any k)

$$\Delta T_{\text{angle,opt}} = \frac{1}{Q_{22}^{(k)}}\frac{\left[Q_{16}^{(k)}Q_{22}^{(k)} - Q_{12}^{(k)}Q_{26}^{(k)}\right]\epsilon_{11}^{\text{mech}}}{Q_{16}^{(k)}\mu_\alpha^{(k)} + Q_{26}^{(k)}\mu_\beta^{(k)} + Q_{66}^{(k)}\mu_{\alpha\beta}^{(k)}} \tag{59}$$

VII. Numerical Results and Discussion

The optimal algorithms outlined in this paper have been applied to three different graphite/epoxy laminates, $[90/0]_S$, $[\pm 45]_S$, and

$[+15/-45/0]_S$ lay-ups. The material properties of each ply are

$$E_{11} = 138 \times 10^6 \text{ kN/m}^2$$

$$E_{22} = E_{33} = 14.5 \times 10^6 \text{ kN/m}^2$$

$$G_{12} = G_{13} = G_{23} = 5.86 \times 10^6 \text{ kN/m}^2$$

$$\nu_{12} = \nu_{13} = \nu_{23} = 0.21$$

$$\mu_L = 0.2 \times 10^{-6} 1/°\text{F}$$

$$\mu_T = \mu_3 = 16 \times 10^{-6} 1/°\text{F}$$

$$t = 0.135 \text{ mm (ply thickness)}$$

Each of the laminates was first subjected to a uniaxial loading within its first-ply-failure strength limit. For the given load, optimal temperature gradients were obtained using the various optimization schemes. These optimal temperature results were then incorporated into calculation of interlaminar stresses under the combined thermomechanical loading. For this purpose, a global-local-thermomechanical stress program called INTGLTM was utilized. This program is based on an assumed stress method and the principle of minimum complementary energy and has been developed at the Center of Excellence for Computational Modeling of Aircraft Structures at the Georgia Institute of Technology. For details of the method, see Ref. 12. Since the program includes effects of both the global and local mismatches, both the results from the global and combined global-local optimizations can be incorporated and verified. Unless indicated otherwise, all of the results are from the global optimization with $\alpha = \beta = 1$.

The first case is the $[90/0]_S$ laminate. As indicated previously, both the global and global-local optimization lead to the same optimal results for a cross-ply laminate. This is also true of the next case, $[\pm 45]_S$ ply laminate. Figure 2 shows the ratio of σ_{33} (or σ_{23}) as a function of the uniform ΔT to σ_{33} (or σ_{23}) for $\Delta T = 0$, at two different loads, $N_{11} = 50$ and 100 kN/M for the $[90/0]_S$ laminate. Since it was assumed that the material properties are invariant under the thermal gradients, all of the stress variations here are seen to be linear functions of the temperature. Also, for positive loads, the slopes are negative and inversely proportional to the load levels. When subjected to a mechanical extension, the transverse normal stress $\tilde{\sigma}_{22}$ in the far field will be in compression in the 90-deg ply and tension in the 0-deg ply, with the same magnitude of the stress in both plies. However, the magnitude of compressive strain in the 90-deg ply is smaller than that of tensile strain in the 0-deg ply due to different magnitudes of Poisson's ratios in these plies. In such a situation, since the graphite/epoxy uniply has a thermal expansion coefficient much smaller in its longitudinal direction than in its transverse direction, it is necessary to heat up the whole laminate to reduce σ_{22} and, consequently, all other stresses. Thus, for $N_{11} = 100$ kN/M, which represents 65% of the maximum failure load of the laminate, $\Delta T = 30°$F will completely eliminate all of the interlaminar stresses. If it is only necessary to attenuate the stresses below the ratio of 1, one can settle for a ΔT between 0 and 60°F. Figures 3 and 4 show through-thickness distributions, predicted by the program INTGLTM, of $\bar{\sigma}_{33}$ at 0.8% laminate thicknesses and $\bar{\sigma}_{23}$ at 5.6% laminate thicknesses from the free edge, after applying a temperature gradient of 25° F along with the mechanical loading, $N_{11} = 100$ kN/M. Note that this temperature difference is close to the $\Delta T_{\text{optimal}} = 30°$F. For this temperature difference the stresses have been reduced by a factor of 6, but have not entirely disappeared. Only applying the optimal temperature gradient would have completely eliminated these stresses.

The next case is the $[\pm 45]_S$ laminate. Figure 5 represents the ratio of interlaminar stress σ_{13} as a function of the uniform ΔT to σ_{13} for $\Delta T = 0$, at two different loads, $N_{11} = 27.5$ and 55 kN/M. As in the $[90/0]_S$ laminate, for the angle-ply laminate the stress reductions are a linear function of ΔT, with slopes inversely proportional to the load levels. The slopes of the angle-ply laminate are, however, positive. For an applied mechanical extension, the angle-ply laminate develops only the shear stress $\tilde{\sigma}_{12}$ in the far field. The shear stress and

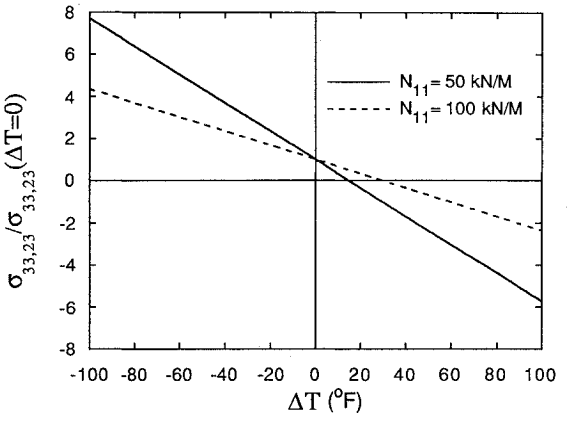

Fig. 2 Graphite/epoxy $[90/0]_S$; $\sigma_{33,23}/\sigma_{33,23}$ ($\Delta T = 0$) vs ΔT at 90/0 interface.

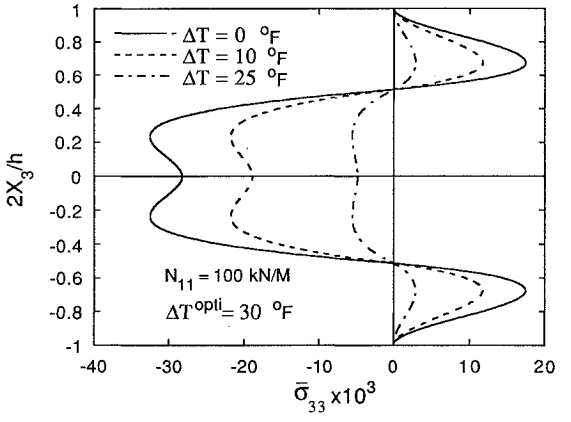

Fig. 3 Graphite/epoxy $[90/0]_S$; $\bar{\sigma}_{33}$ vs $\bar{X}_3$ at 0.8% laminate thickness from the free edge.

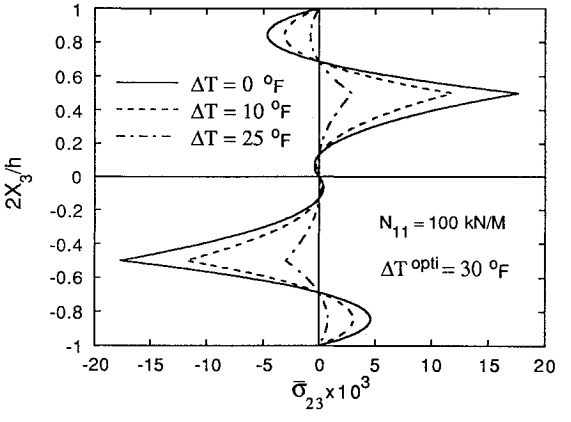

Fig. 4 Graphite/epoxy $[90/0]_S$; $\bar{\sigma}_{23}$ vs $\bar{X}_3$ at 5.6% laminate thickness from the free edge.

the corresponding shear strain will be negative and positive in the 45-deg and −45-deg ply, respectively, with the same magnitudes of the stress and strain in both plies. Once again, because of the different magnitudes of thermal expansion coefficients in its material axes, for a positive temperature difference the graphite/epoxy laminate will have a negative and a positive thermal shear strain in the 45-deg and −45-deg ply, respectively. Hence, it is necessary to cool down the whole laminate and cancel the mechanical extension effect to reduce the stress levels. Thus, for $N_x = 55$ kN/M, which represents 49% of the maximum failure load of the laminate, $\Delta T = -200°$F will completely eliminate the interlaminar stress σ_{13}. Note that according to Eq. (9), this temperature value could mean either heating or cooling depending on the zero residual temperature and the ambient temperature. To give an example, if a composite structure is operating at $T_{\text{ambient}} = -40°$F and its $T_{\text{zero}} = 300°$F, the structure needs to be heated up by 140°F, i.e., its absolute temperature must be 100°F

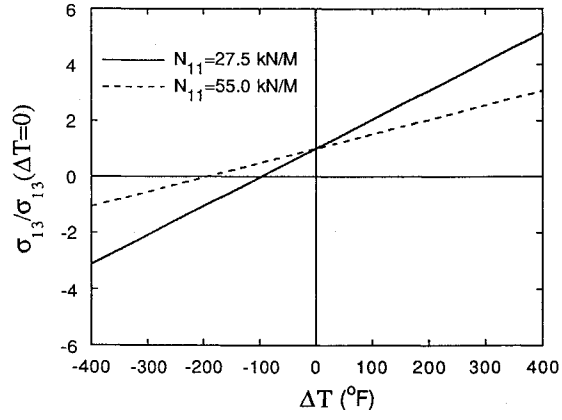

Fig. 5 Graphite/epoxy $[\pm 45]_S$; σ_{13}/σ_{13} ($\Delta T = 0$) vs ΔT at +45/ − 45 interface.

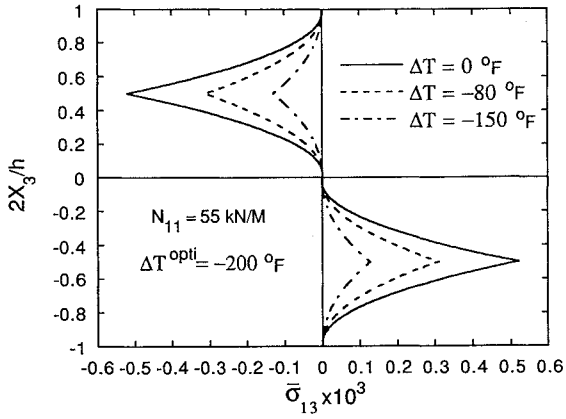

Fig. 6 Graphite/epoxy $[\pm 45]_S$; $\bar{\sigma}_{13}$ vs $\bar{X}_3$ at 0.8% laminate thickness from the free edge.

to eliminate all of the stresses. Figure 6 shows the through-thickness distribution of $\bar{\sigma}_{13}$ near the free edge, after applying a temperature gradient of −150°F along with the mechanical loading, $N_{11} = 55$ kN/M. For this temperature difference the stress has been reduced by a factor of 4, but has not disappeared completely.

The last case is the $[+15/-45/0]_S$ laminate. Figures 7–9 show distributions of various interlaminar stresses after applying the global optimal temperature distribution [designated as $\Delta T_g(x_3)$], $\Delta T^{(1,7)} = -24.8$°F, $\Delta T^{(2,6)} = -35.8$°F, $\Delta T^{(3,5)} = -37.8$°F, and $\Delta T^{(4)} = -28.6$°F, along with the mechanical loading $N_{11} = 20$ kN/M, which represents 2.7% of the maximum failure load. Also shown are two sets of results from the combined global-local optimizations [designated as $\Delta T_{g-l1}(x_3)$ and $\Delta T_{g-l2}(x_3)$]; $\Delta T_{g-l1}(x_3)$ was obtained by setting $\alpha = \beta = 1$ and $\gamma = 0$, $\rho = 1 \times 10^{12}$, and $r^2 = 1.0$. The resulting temperature distribution is $\Delta T^{(1,7)} = -15.48$°F, $\Delta T^{(2,6)} = -43.08$°F, $\Delta T^{(3,5)} = -20.63$°F, and $\Delta T^{(4)} = -34.56$°F; $\Delta T_{g-l2}(x_3)$ was obtained by setting $\alpha = 1$ and $\beta = 0$ and $\gamma = 1 \times 10^{12}$, $\rho = 0$, and $r^2 = 0.3$. The resulting temperature distribution is $\Delta T^{(1,7)} = -10.10$°F, $\Delta T^{(2,6)} = -12.71$°F, $\Delta T^{(3,5)} = -15.56$°F, and $\Delta T^{(4)} = -22.74$°F. Thus, in ΔT_{g-l1}, most weighting is given to σ_{12} and σ_{13}, whereas in ΔT_{g-l2} only σ_{22}, σ_{33}, and σ_{23} are weighted. It is noted that none of the optimal temperature distributions obtained are uniform throughout the laminate thickness. The optimal distributions are also negative throughout the thickness. As expected, it is ΔT_{g-l1} that decreases the interlaminar shear stress σ_{13} most, whereas for ΔT_{g-l2} the interlaminar normal and shear stresses σ_{33} and σ_{33} are reduced most. On the other hand, for ΔT_g the reduction is relatively uniform in all of the interlaminar stresses. However, since σ_{13} has an order of magnitude higher than either of σ_{33} or σ_{23}, it may be desirable to apply ΔT_{g-l1} for this particular lay-up.

As a final note, it is mentioned that, in all of the cases investigated in this paper, the failure loads of the laminates when subjected to optimal temperature gradients have not changed significantly from

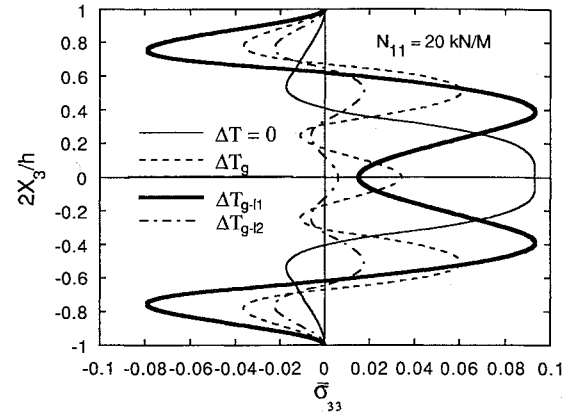

Fig. 7 Graphite/epoxy $[15/-45/0]_S$; $\bar{\sigma}_{33}$ vs $\bar{X}_3$ at 0.8% laminate thickness from the free edge.

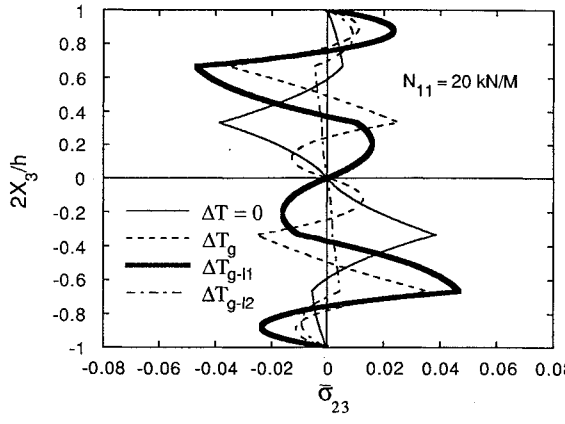

Fig. 8 Graphite/epoxy $[15/-45/0]_S$; $\bar{\sigma}_{23}$ vs $\bar{X}_3$ at 5.6% laminate thickness from the free edge.

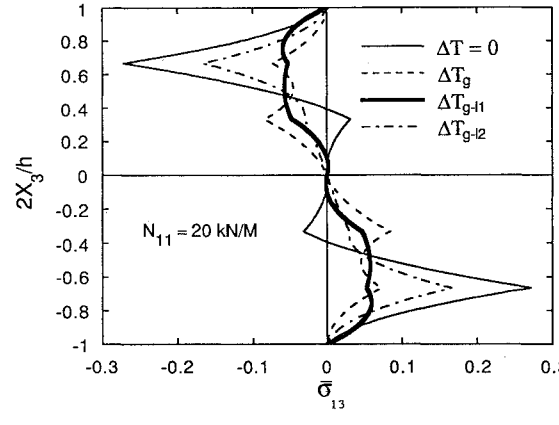

Fig. 9 Graphite/epoxy $[15/-45/0]_S$; $\bar{\sigma}_{13}$ vs $\bar{X}_3$ at 0.8% laminate thickness from the free edge.

their original values, according to the first-ply failure based upon the maximum stress criterion. To give specific percentages of change, the $[90/0]_S$ laminate with the uniform $\Delta T = 25$°F has increased its normal failure load by 16%, whereas the $[\pm 45]_S$ laminate with $\Delta T = -150$°F has decreased it by 35%. For the $[+15/-45/0]_S$ laminate, the change was negligible.

VIII. Conclusions

In this research, analytical solutions of optimal temperature gradients to control interlaminar stresses near the straight free edges of composite laminates have been sought and applied. The optimal temperature gradients are in the through-thickness direction and are obtained by minimizing objective functions that are strictly dependent upon the far-field properties. Through the application of these temperature distributions, all of the interlaminar stresses are minimized in an optimum sense. However, it is more likely that one

may consider applying "pseudo-optimal" temperatures to reduce the stresses below certain threshold levels. In this case, it may be necessary to include constraints in the optimization scheme. It was shown that for both the cross-ply and angle-ply laminates uniform temperature rises or drops can eliminate all of the interlaminar stresses. The nonuniformity of the results for other types of laminates, however, is unavoidable, and it is necessary to heat or cool each lamina with different amounts of temperature. This may be a difficult task for a thin laminate but is certainly possible for thick ones. Most of the optimal temperature gradients obtained here seem feasible in that their distributions are not extremely high or low or abrupt and do not conflict much with the normal failure strengths of the laminates.

As future work, the assumption that each lamina is represented by a linear temperature gradient can be relaxed by using a higher order approximation of the temperature distribution. As indicated earlier, however, such a temperature distribution can be validated only by considering the heat transfer equations and boundary conditions. Second, one can formulate other types of constrained optimization problems in which a set of design objectives, such as normal failure load and laminate stiffness, are set prior to the optimization. Third, it would be interesting to see the effects of material property changes with temperature on the optimal temperature distribution. However, since the suggested active thermal control of the interlaminar stresses would be performed only intermittently in a transient fashion, incorporation of such temperature changes into the present formulations should not be regarded as an absolute requirement. Lastly, one has to devise an active control mechanism that can efficiently realize the concepts and results of the optimal control algorithms that have been suggested in the present paper. One such experimental work is documented in Ref. 8.

Appendix: Thermal Coefficients of Stresses

In all of the equations given in the following text, $(\cdot)_{,i}$ represents a partial derivative with respect to the ith temperature difference $\Delta T^{(i)}$.

The thermal coefficients in Eqs. (13) and (14) are defined as follows:

$$a_{A0i}^{(k)} \equiv A_{01,i}^{(k)}$$

$$= \left[Q_{11}^{(k)}A_{11}^{-1} + Q_{12}^{(k)}A_{12}^{-1} + Q_{16}^{(k)}A_{13}^{-1}\right]N_{11,i}^{T} + \left[Q_{11}^{(k)}A_{12}^{-1} + Q_{12}^{(k)}A_{22}^{-1} + Q_{16}^{(k)}A_{23}^{-1}\right]N_{22,i}^{T} + \left[Q_{11}^{(k)}A_{13}^{-1} + Q_{12}^{(k)}A_{23}^{-1} + Q_{16}^{(k)}A_{33}^{-1}\right]N_{12,i}^{T} + \left[Q_{11}^{(k)}B_{11}^{-1} + Q_{12}^{(k)}B_{12}^{-1} + Q_{16}^{(k)}B_{13}^{-1}\right]M_{11,i}^{T} + \left[Q_{11}^{(k)}B_{12}^{-1} + Q_{12}^{(k)}B_{22}^{-1} + Q_{16}^{(k)}B_{23}^{-1}\right]M_{22,i}^{T} + \left[Q_{11}^{(k)}B_{13}^{-1} + Q_{12}^{(k)}B_{23}^{-1} + Q_{16}^{(k)}B_{33}^{-1}\right]M_{12,i}^{T} + \left[Q_{11}^{(k)}\mu_{\alpha}^{(k)} + Q_{12}^{(k)}\mu_{\beta}^{(k)} + Q_{16}^{(k)}\mu_{\alpha\beta}^{(k)}\right]\frac{1}{t^{(k)}}\left[z^{(k+1)}\delta_{ki} - z^{(k)}\delta_{(k+1)i}\right]$$

$$a_{B0i}^{(k)} \equiv B_{01,i}^{(k)} = \text{same as } a_{A0i}^{(k)} \text{ with } Q_{12}^{(k)}, Q_{22}^{(k)}, Q_{26}^{(k)}$$

$$a_{C0i}^{(k)} \equiv C_{01,i}^{(k)} = \text{same as } a_{A0i}^{(k)} \text{ with } Q_{16}^{(k)}, Q_{26}^{(k)}, Q_{66}^{(k)}$$

and

$$a_{A1i}^{(k)} \equiv A_{11,i}^{(k)}$$

$$= \left[Q_{11}^{(k)}B_{11}^{-1} + Q_{12}^{(k)}B_{12}^{-1} + Q_{16}^{(k)}B_{13}^{-1}\right]N_{11,i}^{T} + \left[Q_{11}^{(k)}B_{12}^{-1} + Q_{12}^{(k)}B_{22}^{-1} + Q_{16}^{(k)}B_{23}^{-1}\right]N_{22,i}^{T} + \left[Q_{11}^{(k)}B_{13}^{-1} + Q_{12}^{(k)}B_{23}^{-1} + Q_{16}^{(k)}B_{33}^{-1}\right]N_{12,i}^{T} + \left[Q_{11}^{(k)}D_{11}^{-1} + Q_{12}^{(k)}D_{12}^{-1} + Q_{16}^{(k)}D_{13}^{-1}\right]M_{11,i}^{T} + \left[Q_{11}^{(k)}D_{12}^{-1} + Q_{12}^{(k)}D_{22}^{-1} + Q_{16}^{(k)}D_{23}^{-1}\right]M_{22,i}^{T} + \left[Q_{11}^{(k)}D_{13}^{-1} + Q_{12}^{(k)}D_{23}^{-1} + Q_{16}^{(k)}D_{33}^{-1}\right]M_{12,i}^{T} - \left[Q_{11}^{(k)}\mu_{\alpha}^{(k)} + Q_{12}^{(k)}\mu_{\beta}^{(k)} + Q_{16}^{(k)}\mu_{\alpha\beta}^{(k)}\right]\frac{1}{t^{(k)}}\left[\delta_{ki} - \delta_{(k+1)i}\right]$$

$$a_{B1i}^{(k)} \equiv B_{11,i}^{(k)} = \text{same as } a_{A1i}^{(k)} \text{ with } Q_{12}^{(k)}, Q_{22}^{(k)}, Q_{26}^{(k)}$$

$$a_{C1i}^{(k)} \equiv C_{11,i}^{(k)} = \text{same as } a_{A1i}^{(k)} \text{ with } Q_{16}^{(k)}, Q_{26}^{(k)}, Q_{66}^{(k)}$$

$$(i = 1, 2, \ldots, N+1, k = 1, 2, \ldots, N)$$

The coefficients in Eqs. (17) and (18) are defined as

$$a_{11i}^{(k)} = A_{11}^{-1}N_{11,i}^{T} + A_{12}^{-1}N_{22,i}^{T} + A_{13}^{-1}N_{12,i}^{T} + B_{11}^{-1}M_{11,i}^{T} + B_{12}^{-1}M_{22,i}^{T} + B_{13}^{-1}M_{12,i}^{T} - \frac{\mu_{\alpha}^{(k)}}{t^{(k)}}\left\{[z - z^{(k+1)}]\delta_{ki} - [z - z^{(k)}]\delta_{(k+1)i}\right\}$$

$$a_{22i}^{(k)} = A_{12}^{-1}N_{11,i}^{T} + A_{22}^{-1}N_{22,i}^{T} + A_{23}^{-1}N_{12,i}^{T} + B_{12}^{-1}M_{11,i}^{T} + B_{22}^{-1}M_{22,i}^{T} + B_{23}^{-1}M_{12,i}^{T} - \frac{\mu_{\beta}^{(k)}}{t^{(k)}}\left\{[z - z^{(k+1)}]\delta_{ki} - [z - z^{(k)}]\delta_{(k+1)i}\right\}$$

$$a_{12i}^{(k)} = A_{13}^{-1}N_{11,i}^{T} + A_{23}^{-1}N_{22,i}^{T} + A_{33}^{-1}N_{12,i}^{T} + B_{13}^{-1}M_{11,i}^{T} + B_{23}^{-1}M_{22,i}^{T} + B_{33}^{-1}M_{12,i}^{T} - \frac{\mu_{\alpha\beta}^{(k)}}{t^{(k)}}\left\{[z - z^{(k+1)}]\delta_{ki} - [z - z^{(k)}]\delta_{(k+1)i}\right\}$$

The coefficients inside the summations of Eq. (52) are defined as

$$\delta(a_{\nu 12})_i(k, 2) \equiv \left[\delta\nu_{12E}(k)\epsilon_b^{(k)}\right]_{,i}$$

$$= \delta\nu_{12}(k, 2)\epsilon_{b,i}^{(k)\theta} - \delta a_{\nu\mu}(k)\delta_{(k+1)i}$$

$$\delta(a_{\eta 12,1})_i(k, 2) \equiv \left[\delta\eta_{12,1E}(k)\epsilon_b^{(k)}\right]_{,i}$$

$$= \delta\eta_{12,1}(k, 2)\epsilon_{b,i}^{(k)\theta} - \delta a_{\eta\mu}(k)\delta_{(k+1)i}$$

where $\epsilon_b^{(k)\theta}$ is the thermal part of the total strain $\epsilon_b^{(k)}$, and

$$\epsilon_{b,i}^{(k)\theta} \equiv A_{11}^{-1}N_{11,i}^{T} + A_{12}^{-1}N_{22,i}^{T} + A_{13}^{-1}N_{12,i}^{T} + B_{11}^{-1}M_{11,i}^{T} + B_{12}^{-1}M_{22,i}^{T} + B_{13}^{-1}M_{12,i}^{T} + z^{(k+1)}\left(B_{11}^{-1}N_{11,i}^{T} + B_{12}^{-1}N_{22,i}^{T} + B_{13}^{-1}N_{12,i}^{T} + D_{11}^{-1}M_{11,i}^{T} + D_{12}^{-1}M_{22,i}^{T} + D_{13}^{-1}M_{12,i}^{T}\right)$$

The terms $\delta(a_{\nu 12})_i(k, 1)$ and $\delta(a_{\eta 12,1})_i(k, 1)$ are defined in a similar fashion at the top of the kth ply.

The thermal load derivatives in all of the preceding equations are defined as

$$N_{11,i}^{T} = \tfrac{1}{2}\left[Q_{11}^{(i)}\mu_{\alpha}^{(i)} + Q_{12}^{(i)}\mu_{\beta}^{(i)} + Q_{16}^{(i)}\mu_{\alpha\beta}^{(i)}\right]t^{(i)} + \tfrac{1}{2} \times \left[Q_{11}^{(i-1)}\mu_{\alpha}^{(i-1)} + Q_{12}^{(i-1)}\mu_{\beta}^{(i-1)} + Q_{16}^{(i-1)}\mu_{\alpha\beta}^{(i-1)}\right]t^{(i-1)}$$

$$N_{22,i}^{T} = \tfrac{1}{2}\left[Q_{12}^{(i)}\mu_{\alpha}^{(i)} + Q_{22}^{(i)}\mu_{\beta}^{(i)} + Q_{26}^{(i)}\mu_{\alpha\beta}^{(i)}\right]t^{(i)} + \tfrac{1}{2} \times \left[Q_{12}^{(i-1)}\mu_{\alpha}^{(i-1)} + Q_{22}^{(i-1)}\mu_{\beta}^{(i-1)} + Q_{26}^{(i-1)}\mu_{\alpha\beta}^{(i-1)}\right]t^{(i-1)}$$

$$N_{12,i}^{T} = \tfrac{1}{2}\left[Q_{16}^{(i)}\mu_{\alpha}^{(i)} + Q_{26}^{(i)}\mu_{\beta}^{(i)} + Q_{66}^{(i)}\mu_{\alpha\beta}^{(i)}\right]t^{(i)} + \tfrac{1}{2} \times \left[Q_{16}^{(i-1)}\mu_{\alpha}^{(i-1)} + Q_{26}^{(i-1)}\mu_{\beta}^{(i-1)} + Q_{66}^{(i-1)}\mu_{\alpha\beta}^{(i-1)}\right]t^{(i-1)}$$

$$M_{11,i}^{T} = \tfrac{1}{6}\left[Q_{11}^{(i)}\mu_{\alpha}^{(i)} + Q_{12}^{(i)}\mu_{\beta}^{(i)} + Q_{16}^{(i)}\mu_{\alpha\beta}^{(i)}\right]t^{(i)}[3z^{(i)} - t^{(i)}] + \tfrac{1}{6}\left[Q_{11}^{(i-1)}\mu_{\alpha}^{(i-1)} + Q_{12}^{(i-1)}\mu_{\beta}^{(i-1)} + Q_{16}^{(i-1)}\mu_{\alpha\beta}^{(i-1)}\right] \times t^{(i-1)}[3z^{(i-1)} - 2t^{(i-1)}]$$

$$M_{22,i}^{T} = \tfrac{1}{6}\left[Q_{12}^{(i)}\mu_{\alpha}^{(i)} + Q_{22}^{(i)}\mu_{\beta}^{(i)} + Q_{26}^{(i)}\mu_{\alpha\beta}^{(i)}\right]t^{(i)}[3z^{(i)} - t^{(i)}] + \tfrac{1}{6}\left[Q_{12}^{(i-1)}\mu_{\alpha}^{(i-1)} + Q_{22}^{(i-1)}\mu_{\beta}^{(i-1)} + Q_{26}^{(i-1)}\mu_{\alpha\beta}^{(i-1)}\right] \times t^{(i-1)}[3z^{(i-1)} - 2t^{(i-1)}]$$

$$M_{12,i}^{T} = \tfrac{1}{6}\left[Q_{16}^{(i)}\mu_{\alpha}^{(i)} + Q_{26}^{(i)}\mu_{\beta}^{(i)} + Q_{66}^{(i)}\mu_{\alpha\beta}^{(i)}\right]t^{(i)}[3z^{(i)} - t^{(i)}] + \tfrac{1}{6}\left[Q_{16}^{(i-1)}\mu_{\alpha}^{(i-1)} + Q_{26}^{(i-1)}\mu_{\beta}^{(i-1)} + Q_{66}^{(i-1)}\mu_{\alpha\beta}^{(i-1)}\right] \times t^{(i-1)}[3z^{(i-1)} - 2t^{(i-1)}]$$

where ($i = 2, 3, \ldots, N$; for $i = 1, N+1$, the $(i-1)$, and (i) terms, respectively, are not included).

Acknowledgment

This work was supported by a grant from the Federal Aviation Administration to the Center of Excellence for Computational Modeling of Aircraft Structures at Georgia Institute of Technology.

References

[1]Pagano, N. J., and Pipes, R. B., "Some Observations on the Interlaminar Strength of Composite Laminates," *International Journal of Mechanical Sciences*, Vol. 15, No. 8, 1973, pp. 679–688.

[2]Pagano, N. J., and Lackman, L. M., "Prevention of Delamination of Composite Laminates," *AIAA Journal*, Vol. 13, No. 3, 1975, pp. 399–401.

[3]Mignery, L. A., Tan, T. M., and Sun, C. T., "The Use of Stitching to Suppress Delamination in Laminated Composites," *Delamination and Debonding of Materials*, ASTM Special Technical Publication 876, edited by W. S. Johnson, ASTM, Philadelphia, PA, 1985, pp. 371–385.

[4]Herakovich, C. T., "On Thermal Edge Effects in Composite Laminates," *International Journal of Mechanical Sciences*, Vol. 18, No. 3, 1976, pp. 129–134.

[5]Wang, A. S. D., and Crossman, F. W., "Edge Effects on Thermally Induced Stresses in Composite Laminates," *Journal of Composite Materials*, Vol. 11, July 1977, pp. 300–312.

[6]Webber, J. P. H., and Morton, S. K., "An Analytical Solution for the Thermal Stresses at the Free Edges of Laminated Plates," *Composite Sciences and Technology*, Vol. 46, No. 2, 1993, pp. 175–185.

[7]Kim, T., and Atluri, S. N., "Optimal Temperature Distributions for Control of Interlaminar Stresses in Composite Laminates" AIAA/ASME/ASCE/AHS/ASC 35th Structures, Structural Dynamics, and Materials Conference, AIAA Paper 94-1635, Hilton Head, SC, April 1994.

[8]Kim, T., Steadman, D., Hanagud, S. V., and Atluri, S. N., "Active Control of Interlaminar Stresses in Laminated Composites by Through-Thickness Thermal Gradients," *Proceedings of the North American Smart Structures and Materials Conference* (San Diego, CA), Feb. 1995.

[9]Jones, R. M., *Mechanics of Composite Materials*, McGraw–Hill, New York, 1975.

[10]Rose, C. A., "An Approximate Solution for Interlaminar Stresses in Laminated Composite," Ph.D. Thesis, Applied Mechanics Program, Univ. of Virginia, Charlottesville, VA, 1992.

[11]Rose, C. A., and Herakovich, C. T., "An Approximate Solution for Interlaminar Stresses in Composite Laminates," *Composites Engineering*, Vol. 3, No. 3, 1993, pp. 271–285.

[12]Kim, T., and Atluri, S. N., "Analysis of Edge Stresses in Composite Laminates Under Combined Thermo-Mechanical Loading, Using a Complementary Energy Approach," *Computational Mechanics* (to be published).